Stress Relaxation of Branched Polymers

Jung Hun Lee, Lewis J. Fetters, and Lynden A. Archer*

School of Chemical and Biomolecular Engineering, Cornell University, Ithaca, New York 14853

Received August 23, 2005; Revised Manuscript Received October 5, 2005

ABSTRACT: Stress relaxation dynamics of model branched homopolymers with a range of architectures (A_2**B** (T-shaped) and A$\mathbf{B}_2$ (Y-shaped) asymmetric stars, A$\mathbf{B}_n$ (combs), $\mathbf{B}_2$-A-$\mathbf{B}_2$ (H-shaped), and $\mathbf{B}_3$-A-$\mathbf{B}_3$ (pom-poms)) are studied using a tube-based theory to evaluate a recent proposal for branch point motion in *hierarchically* relaxing branched molecules. This model contends that if the random coil size $R_{g,\mathbf{B}}$ of relaxed **B** arms connected via a branch point to an unrelaxed Z_A-mer polymer backbone is larger than the equilibrium tube diameter a, the branch point can only move a small distance $\delta = (ap)$ of order $a/\sqrt{Z_A}$ during each relaxation cycle of the arms. When this prediction is integrated into tube models for branched molecules, it yields a self-consistent theory suitable for describing linear viscoelasticity (LVE) of any branched polymer system. Without artifices, such as arbitrary adjustments of the measured molecular weights, arm functionality, or dilution exponent, we find that this theory yields LVE predictions that are consistent with experimental data from many groups.

Introduction

The success of the reptation theory in describing rheological properties of linear polymers[1,2] and the well-known commercial importance of branched polyolefins[3−6] have motivated efforts by many groups to develop a tube model framework for branched polymers.[7−9] The dynamic dilution (DD) assumption,[9−11] wherein the already relaxed portion of a branched polymer chain acts as an effective solvent for the unrelaxed portions, provides a simple and efficient way to integrate the effect of faster relaxing side branches on dynamics of slower relaxing molecular backbone segments and is now regarded as a vital component in any theory for branched polymer dynamics.[11−16] There are nonetheless longstanding theoretical and recent experimental puzzles that will undoubtedly lead to deeper molecular-level understanding of DD and its relationship to constraint-release processes in simple bidisperse blends.[17−20]

There are two additional assumptions commonly made in tube-based theories for branched molecules. (i) Branched polymers relax *hierarchically*. Thus, the effective backbone between two branch points becomes mobile after relaxation of the arms is complete. Used in conjunction with DD, the slow-relaxing backbone can be visualized as an effective linear chain that relieves stress by reptation. (ii) Branch points carry additional drag friction caused by already relaxed side branches. Hence, terminal dynamics of branched polymers are controlled by reptative motion of this backbone with friction concentrated at the relaxed blobs. For a generic A_2**B** asymmetric star polymer with $M_{w,A} \gg M_{w,\mathbf{B}}$ or a $\mathbf{B}_n$-A-$\mathbf{B}_n$ multiarm pom-pom, the blob friction, $\zeta_{bp} \approx kT(\tau_{a,\mathbf{B}}/a^2)$ is generally much larger than the tube Rouse friction on the bare backbone, $\zeta_T \approx kT(Z_{A,R}\tau_e/a^2)$. The diffusivity of the branch point

$$D_{bp} = \delta^2/2\tau_{a,\mathbf{B}} \tag{1}$$

therefore sets the fundamental time constant for reptation of the A backbone. Here, $Z_{A,R}$ is the number of entanglements in the unrelaxed backbone segment connected to the branch point, $\tau_{a,\mathbf{B}}$ is the **B** arm relaxation time, a is the diameter of the tube in which the backbone relaxes, and $\delta = (ap)$ is the unknown distance the branch point moves during each relaxation cycle of the **B** arms. If the random coil size of the relaxed blob at a branched junction (e.g., $R_{g,\mathbf{B}}$ in an A_2**B** asymmetric star polymer) is larger than the tube diameter a, an unknown large number of arm relaxation cycles is expected to expire before the backbone can reptate a distance of order the tube diameter, i.e., without dragging other unrelaxed backbones entangled with it. Thus, the parameter p should itself generally be a function of the arm and backbone molecular weights as well as the architecture of the polymer (e.g., asymmetric star vs pom-pom, see below) under consideration.

Original studies by McLeish and co-workers concluded that a is the bare tube diameter a_0 dilated by relaxation of molecular segments on time scales $t \leq \tau_{a,\mathbf{B}}$ (i.e., $a(\phi_{bb}) = a_0/\phi_{bb}^{2/3}$, where ϕ_{bb} is the volume fraction of backbone segments), and p is a fixed parameter with a value of order 1/6 or 1/12 for entangled $\mathbf{B}_2$-A-$\mathbf{B}_2$ (H-shaped) polymers.[12] Subsequent studies by other authors suggest that a is closer to the undilated tube diameter a_0, and p is in fact a function of architectural details of the polymer.[14−16,21−25] In a recent study, we proposed a simple analytical formula between p and the entanglement density $Z_{A,R}$ of unrelaxed backbone segments, $p^2 = 1/Z_{A,R}$, for asymmetric star polymers.[15] Inserting this formula in eq 1 yields an expression for the branch point diffusivity that takes into account both the localized frictional drag exerted on the branch point by the attached arms and the distributed coupled drag of chains connected with the backbone by entanglements. This expression should therefore be universally valid for all branched molecules.

In a melt of A_2**B** asymmetric star chains $Z_{A,R}/2 = N_{A,R}/N_e < N_A/N_e$, where $N_{A,R}$ is the degree of polymerization of the unrelaxed A arm segment on time scales $t > \tau_{a,\mathbf{B}}$ and N_A is the degree of polymerization of the A arm. The hopping distance is then implicitly dependent on the **B** arm length, through $\tau_{a,\mathbf{B}}$. For a $\mathbf{B}_n$-A-$\mathbf{B}_n$ (multiarm, pom-pom), $Z_{A,R} = Z_A = N_A/N_e$, and p is now independent of arm length and can be obtained directly from the entanglement density of the cross-bar A. In

10.1021/ma051856x CCC: $30.25
Published on Web 11/10/2005

both cases the predicted inverse relationship between p and number of remaining entanglements is in qualitative accord with experimental findings for asymmetric stars,[14] and $\mathbf{B}_3$-A-$\mathbf{B}_3$ pom-pom melts, and solutions.[16,23] Furthermore, when integrated in the tube model of Frischknecht et al. for asymmetric stars,[13] this formula yields a self-consistent tube model suitable for predicting linear viscoelastic properties of all branched polymers.

The objective of the present study is to evaluate the general validity of the branch point hopping formula discussed above. We will use this formula in conjunction with the tube model[12−14] to predict LVE of all *hierarchically* relaxing polymer systems (combs, T-shaped asymmetric stars, $\mathbf{B}_2$-A-$\mathbf{B}_2$ H-shaped, and $\mathbf{B}_3$-A-$\mathbf{B}_3$ pom-poms) for which experimental data are available. Since our goal is to evaluate the generality of this formula, we will ignore corrections due to polydispersity and will use the fundamentally based Colby−Rubinstein dilution exponent[26] throughout. A perhaps obvious question is whether placing a single branch point away from the end of the backbone (as is the case for T-shaped $A_2\mathbf{B}$) or at one end as would be the case for a Y-shaped $A\mathbf{B}_2$ (again with $M_{w,A} \gg M_{w,\mathbf{B}}$) should really produce the same qualitative effect on branch point motion. Specifically, if the unrelaxed backbone contains a free end and a large friction center at the other end, two situations can be imagined. For A not too much larger than **B** the free end is much easier to move than the branch point; the branch point can then be visualized as a fixed tether. In this situation, arm retraction will be the governing mechanism by which the imposed stress on the entire molecule relaxes. On the other hand, if $M_{w,A} \gg M_{w,\mathbf{B}}$, after some period of retraction, the accumulated friction at the free end will become comparable to that of the relaxed blob at the other end, favoring a terminal reptation-like process. LVE studies using Y-shaped asymmetric stars therefore provide a nice complement to work with other branched architectures.

Experiment

A 1,4-polyisoprene Y-shaped asymmetric star polymer was synthesized using anionic techniques under high-vacuum conditions as described earlier.[15] To obtain the Y-shaped polymer with an $A\mathbf{B}_2$ structure, the living long arm A is first added to a large excess of purified linker, CH_3SiCl_3, to produce long arm linkers, CH_3SiACl_2. Excess CH_3SiCl_3 was removed by direct distillation. The living short arms **B** were reacted with the long arm linkers, CH_3SiACl_2, to form the desired Y-shaped asymmetric star polymer $A\mathbf{B}_2$110K. A long arm molecular weight $M_A \sim 110$K and the short arm molecular weight $M_\mathbf{B} \sim 33$K were targeted. These values are selected because the initial backbone length and total molecular weight of $A\mathbf{B}_2$110K are equivalent to those of the T-shaped asymmetric star polymer $A_2\mathbf{B}$73K in the earlier study[15] (see Figure 1). Molecular weights of long and short arms were characterized using a Viscotek size exclusion chromatography (SEC) comprised of four mixed bed columns and equipped with a laser light scattering detector (TDA302), as shown in Table 1. The final product of $A\mathbf{B}_2$110K was obtained by repeated toluene/methanol fractionation (see Figure 2).

Stress relaxation dynamics of $A\mathbf{B}_2$110K were quantified using small-amplitude oscillatory shear measurements. A TA Instruments ARES-LS rheometer with 10 mm and 4 mm diameter parallel plate fixtures was used to measure linear viscoelastic properties at temperatures ranging from −40 to 28 °C. The Ochestrator software was used to derive master curves at a reference temperature $T_{ref} = 28$ °C by a two-dimensional residual minimization technique. The WLF fit for

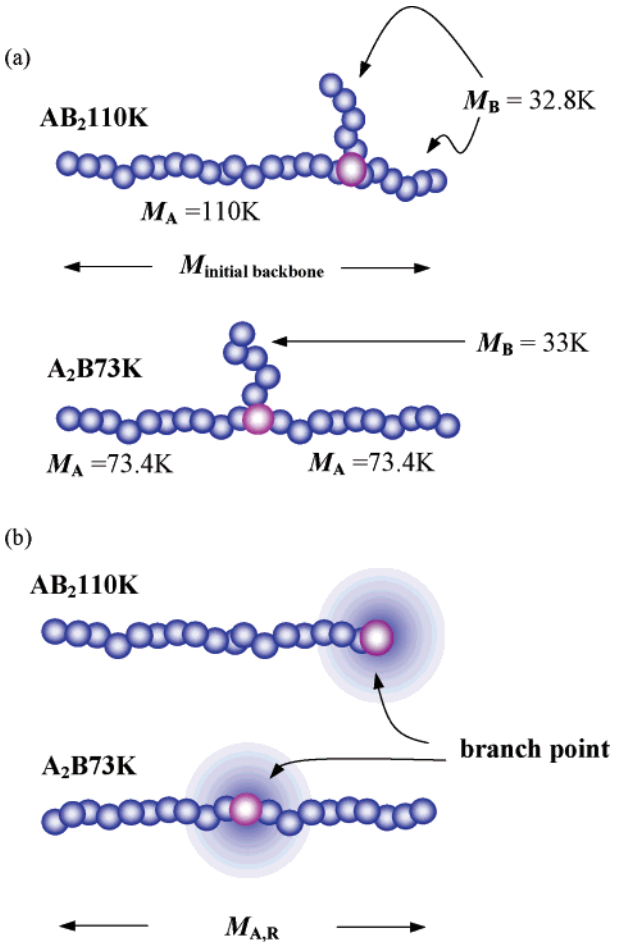

Figure 1. Schematic illustration for (a) T-shaped (A_2B73K) and Y-shaped ($AB_2$110K) asymmetric star polymers with long arm molecular weight M_A and short arm molecular weight M_B. (b) The unrelaxed remaining backbones with the branch point after the relaxation of short arms. The remaining backbone molecular weight is $M_{A,R}$.

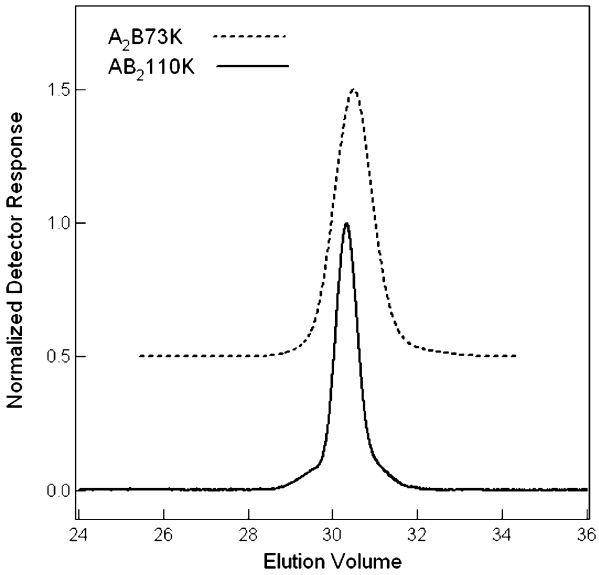

Figure 2. GPC analysis of T-shaped (A_2B73K) and Y-shaped ($AB_2$110K) asymmetric star polymers taken from the final stage of the respective fractionations.

the shifting factor a_T, $\log(a_T) = [-C_1(T - T_{ref})]/[C_2 + T - T_{ref}]$, yields $C_1 = 5.1$ and $C_2 = 145$ [°C], which are similar to the values of $C_1 = 5.0$ and $C_2 = 140$ [°C] for 1,4-polyisoprene asymmetric star polymers.[14]

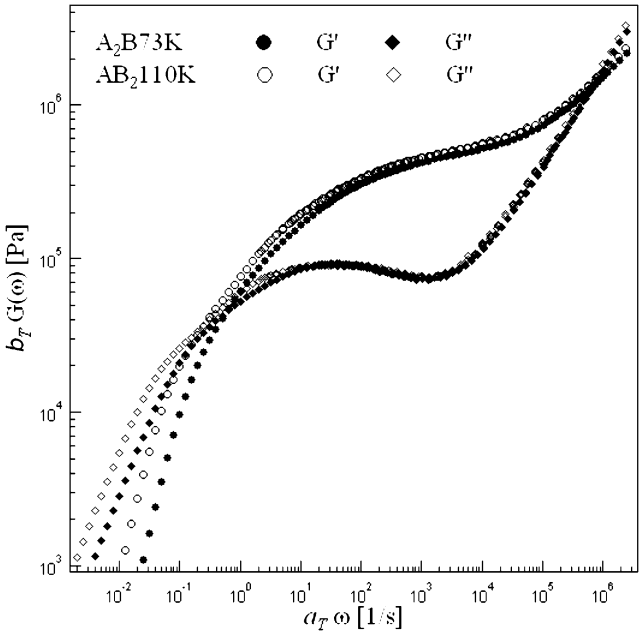

Figure 3. Dynamic moduli, $G'(\omega)$ and $G''(\omega)$, of T-shaped (A_2-B73K) and Y-shaped ($AB_2$110K) asymmetric star polymers.

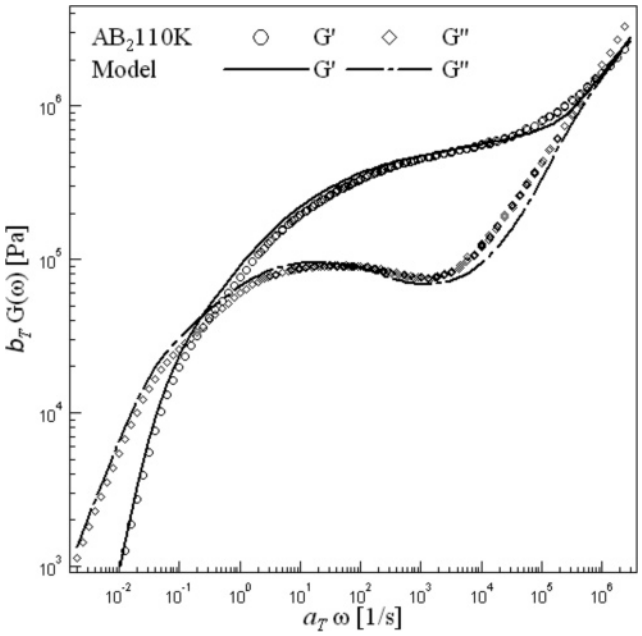

Figure 4. Comparison of experimental and theoretical dynamic moduli, $G'(\omega)$ and $G''(\omega)$, of $AB_2$110K. Symbols are the measured data, and lines are the model predictions.

Results and Discussion

Linear Viscoelasticity of Y-Shaped Asymmetric Star. As illustrated in Figure 1a, the structures of A_2**B**73K and A**B**$_2$110K have nearly identical initial backbones of around 140K. The entanglement densities of the both short arms are large enough to produce starlike dynamics in these asymmetric architectures. Figure 1b illustrates how the dissimilar short arm placements should affect the position of friction centers on the unrelaxed backbone sections on time scales $t > \tau_{a,\mathbf{B}}$. As shown in Figure 3, dynamic storage and loss moduli, $G'(\omega)$ and $G''(\omega)$, of A_2**B**73K and A**B**$_2$110K are quite similar for much of the frequency range, but a slightly slower relaxation of the A**B**$_2$110K polymer is observed in the terminal regime. The shape of the $G''(\omega)$ maximum at the intermediate frequencies is also consistent with expectations for dynamics of two branched structures with similar short arm molecular weight. The obtained material properties of A**B**$_2$110K, the zero shear viscosity $\eta_0 = G''(\omega)/\omega|_{\lim_{\omega\to 0}}$ and the terminal relaxation times as a reciprocal of the frequency $\omega_{\text{crossover}}$ at which $G'(\omega)$ and $G''(\omega)$ cross over prior to the onset of terminal behavior and a reciprocal of $\omega_{\eta''}$ at which $\eta''(\omega) = G'(\omega)/\omega$ manifests a local minimum, are around 2 times larger than those of A_2**B**73K (see Table 1).

As a first test of the proposed formula for p^2, we compare the predicted moduli of A**B**$_2$110K based on $D_{\text{bp}} = (pa_0)^2/2\tau_{a,\mathbf{B}}$ with experimental data in Figure 4. The same model framework proposed in the earlier study[15] is used for predictions. During the short arm relaxation, some parts of long arm also relax. The retraction process of the unrelaxed long arm $Z_{A,R}$ sections continues as contour length fluctuations until the reptative motion of the remaining backbone outcompetes deeper retraction of $Z_{A,R}$ (i.e., when arm retraction of the free end becomes slower than branch point mediated reptative motion, the branch point becomes *mobile* and reptation diffusion dominates terminal relaxation.) The value of p^2 in this Y-shaped polymer is determined self-consistently from the unrelaxed long arm $M_{A,R}$ predicted by the theory and the same model parameters, $M_{\text{ef}} = 4200$ [g/mol], $G_{\text{Nf}} = 0.6$ [MPa], and $\tau_{\text{ef}} = 7.4 \times 10^{-6}$ [s], used in our earlier work.[15] It is evident from the figure that the model quite nicely describes the experimental data, without need for artificially adjusting the polymer molecular weight, changing the dilution exponent, or taking into account the finite polydispersity of the polymer. This simple test indicates the proposed branch point mobility $D_{\text{bp}} = a_0^2/(2\, Z_{A,R}\, \tau_{a,\mathbf{B}})$ is consistently valid for the two extreme possible placement of branch points on a star-shaped molecule. We therefore turn next to more complex systems comprised of multiple branch points placed at variable positions along the backbone contour.

Generalized Model. As discussed earlier, within the dynamic dilution framework, relaxation of side arms occur first and is followed by branch point mediated reptative motion of unrelaxed backbone segments. H-shaped, multiarm, and comb polymers contain a back-

Table 1. Molecular Characterization Information for T- and Y-Shaped Asymmetric Stars

sample	M_n (SEC with LS) [g/mol] (1) short (2) long (3) total	PDI	η_0 [Pa s]	$\omega_{\text{crossover}}$ [1/s]	$\omega_{\eta''\text{max}}$ [1/s]	M in model [g/mol] (1) short (2) long
A_2B73K[15]	(1) 33000	1.01	2.91×10^5	5.75×10^{-1}	1.59×10^{-1}	(1) 33000
	(2) 73400	1.05				(2) 73400
	(3) 169000	1.06				
$AB_2$110K	(1) 32780	1.01	5.69×10^5	2.69×10^{-1}	6.31×10^{-2}	(1) 32800
	(2) 110060	1.03				(2) 110000
	(3) 170060	1.03				

bone $N_{bb} = M_{bb}/M_0$ with q branch points each containing x arms of equal length $N_a = M_a/M_0$. Thus, the volume fraction of arms is $\phi_a = xqM_a/(M_{bb} + xqM_a)$. The entanglement molecular weight[27] $M_e = \rho RT/(5/4)G_N$, the undilated tube diameter $a_0^2 = (M_e/M_0)b^2 = N_e b^2$, and the entanglement equilibration time τ_e are used throughout the analysis. Here, ρ is the density of the polymer, R is the gas constant, T is the absolute temperature, and G_N is the plateau modulus.

In the arm relaxation mode, the effective potential of side arms is given by[11−15]

$$U_a(s_a) = 3Z_a \frac{1 - (1 - \phi_a s_a)^{\alpha+1}[1 + (1 + \alpha)\phi_a s_a]}{\phi_a^2(\alpha + 1)(\alpha + 2)} \quad (2)$$

Here, $Z_a = M_a/M_e$ is the number of entanglements per arm and s_a is a fractional distance from the free end. The outer parts of arm are relaxed by the curvilinear Rouse motion following a relationship $s_a \sim t^{1/4}$, while the motion of inner parts are described by the analytical solution of a first-passage time problem

$$\tau_a(s_a) = \frac{L_a^2}{D_{eff}} \int_0^{s_a} \exp[U(s')] \int_{-\infty}^{s'} \exp[-U(s'')]\, ds''\, ds'$$

with the arm contour length $L_a = N_a b^2/a$ and the effective diffusion constant as twice the Rouse diffusion constant of an arm $D_{eff} = 2D_{c,a}$. The arm relaxation time can then be determined from the *early* fluctuation time and the *late* fluctuation time as follows:[11−15]

$$\tau_{early}(s_a) = \frac{9\pi^3}{16} \tau_e Z_a^4 s_a^4 \quad (3)$$

$$\tau_{late}(s_a) = \sqrt{\frac{\pi^5}{6}} \tau_e Z_a^{3/2} \times \frac{\exp[U_a(s_a)]}{\sqrt{s_a^2(1 - \phi_a s_a)^{2\alpha} + \frac{1}{\phi_a^2}\left(\frac{\phi_a^2(1 + \alpha)}{3Z_a}\right)^{2\alpha/(1+\alpha)} \left(\Gamma\left[\frac{1}{(1 + \alpha)}\right]\right)^{-2}}} \quad (4)$$

$$\tau_a(s_a) = \frac{\tau_{early}(s_a) \exp[U_a(s_a)]}{1 + \tau_{early}(s_a) \exp[U_a(s_a)]/\tau_{late}(s_a)} \quad (5)$$

After the relaxation of arm $\tau_a(s_a = 1)$, the total drag friction on the backbone is the sum of friction from branch points and monomeric friction along the bare backbone, $\zeta_{total} = q\zeta_{bp} + \zeta_{bb} = 2\zeta_{half}$.[14,15] The mobility of backbone is therefore determined from the branch point diffusivity and Rouse diffusivity of backbone segments

$$1/D_{total} = q/D_{bp} + 1/D_{c,bb} = 2/D_{half} \quad (6)$$

The terminal relaxation time of the reptating backbone is determined by $\tau_{rep}(s) = [L_{eff,bb}^2(1 - s)^2]/\pi^2 D_{eff,bb}$, where $L_{eff,bb} = N_{bb}b^2/a(\phi_{bb})$ and $D_{eff,bb} = D_{total}$.[12−15] The effective mobility of the backbone then explicitly depends on the number of branch points. The mobility of branch point is given by eq 1 with $a = a_0$ and $p^2 = 1/Z_{bb}$. In the earlier H-shaped polymer model,[12] the mobility of the branch point is assumed to explicitly depend on the number of arms per branch point. In the limiting case of a symmetric star, this assumption yields an explicit dependence of relaxation time on number of arms, which has not been observed. Here we remove this factor because the number of arms is already implicitly incorporated in the arm relaxation time through its effect on the volume fraction of unrelaxed segments at any instant in time. Thus, the mobility of the branch point contains the effect of the number of arms and arm entanglement density through their effect on $\tau_{a,\mathbf{B}}$ and the effect of the polymer architecture through $p^2 = 1/Z_{bb} = M_e/M_{bb}$.[15]

The arm relaxation and the terminal relaxation are connected by the intermediate fluctuating motion of the unrelaxed backbone.[12,13] This fluctuating motion is described by the two-arm star approximation.[11] In the *early* fluctuation, two situations are anticipated. First, in cases where there are only a small number of branch points (*small q*) per chain (e.g., a H-shaped polymer), the backbone can fluctuate in an analogous manner to a linear polymer, except with an extra damping due to the branch points (or friction blobs). Thus, in this case the branch point executes coordinated motion in the direction set by the backbone. In the case where there are numerous branch points distributed along the backbone (*large q*) such coordinated motion is not possible and the branch points only permit local early fluctuations of the backbone. To evaluate both possibilities, we divide the *early* fluctuation into two modes, small q (Sq) and large q (Lq), and evaluate the effect of each by comparisons with experimental data.

I. Early Fluctuation: Sq Mode. In the small q mode, the backbone executes coordinated fluctuations along its entire length by dragging the q branch points en mass through the effective entanglement network. In this case the backbone mobility contains, as before, $D_{bp,Sq} = (a_0^2/2\tau_a)(1/Z_{bb})$. The *early* fluctuation time, by analogy to a Rouse chain[12,13] $\langle \Delta R^2 \rangle = 2D_R t$, is given by $\tau_{early,Sq}(s_{bb}) = (s_{bb}L_{eff,half})^2/2D_{half}$ where $L_{eff,half} = L_{eff,bb}/2$ and D_{half} from eq 6 with $D_{bp,Sq}$.

II. Early Fluctuation: Lq Mode. In the large q mode branch points only permit local fluctuations of the backbone on small time scales. In this case the branch point-mediated backbone mobility is given by $D_{bp,Lq} = a_0^2/2\tau_a$. The *early* fluctuation time computed from the curvilinear Rouse motion[2,11] $\langle z(t)^2 \rangle = (4/3\pi^{3/2})R_{half}^2(t/\tau_{R,half})^{1/2}$ is then given by $\tau_{early,Lq}(s_{bb}) = (9\pi^3/16)(s_{bb}L_{eff,half}/R_{half})^4\tau_{R,half}$ where $R_{half} = (N_{bb}/2)b^2$, $\tau_{R,half} = R_{half}^2/(3\pi^2 D_{half})$, and D_{half} from eq 6 with $D_{bp,Lq}$.

III. Late Fluctuations. On longer time scales, the half-arm retracts like the arm in a star polymer so the mobility becomes $D_{bp} = (a_0^2/2\tau_a)(1/Z_{bb})$, irrespective of q. The effective potential $U_{bb}(s_{bb})$ of half-arms and the late time $\tau_{late}(s_{bb})$ with $Z_{bb,half} = (M_{bb}/2)/M_e = Z_{bb}/2$ and $D_{eff,half} = 2D_{half}$ from eq 6 are therefore given by[11−13]

$$U_{bb}(s_{bb}) = 3Z_{bb,half}\phi_{bb}^{\alpha} \frac{1 - (1 - s_{bb})^{\alpha+1}[1 + (1 + \alpha)s_{bb}]}{(\alpha + 1)(\alpha + 2)} \quad (7)$$

$$\tau_{late,bb}(s_{bb}) = \frac{L_{eff,half}^2}{D_{eff,half}} \sqrt{[2\pi]/[3Z_{bb,half}\phi_{bb}^{\alpha}]} \times [\exp[U_{bb}(s_{bb})]]/\left[3Z_{bb,half}\phi_{bb}^{\alpha} \times \sqrt{s_{bb}^2(1 - s_{bb})^{2\alpha} + \left(\frac{(1 + \alpha)}{3Z_{bb,half}\phi_{bb}^{\alpha}}\right)^{2\alpha/(1+\alpha)} \left(\Gamma\left[\frac{1}{(1 + \alpha)}\right]\right)^{-2}}\right] \quad (8)$$

Thus, the half-arm relaxation time is determined from

the early time ($i = Sq$ or Lq) and the late fluctuation time as[11−13]

$$\tau_{bb}(s_{bb}) = \frac{\tau_{early,i}(s_{bb})\exp[U_{bb}(s_{bb})]}{1 + \tau_{early,i}(s_{bb})\exp[U_{bb}(s_{bb})]/\tau_{late,bb}(s_{bb})} \quad (9)$$

Thus, the current approach contains four main relaxation modes: a high-frequency Rouse mode,[27] the arm relaxation, the early and late fluctuation modes, and terminal relaxation. The terminal relaxation time of the backbone can now be calculated as $\tau_{rep}(s_d)$, where s_d is determined from the criterion $\tau_{rep}(s_{bb}) = \tau_{bb}(s_{bb})$. The relaxation modulus for the combination of modes is written as $G(\omega) = G_{high-Rouse}(\omega) + G_{arm}(\omega) + G_{fluc}(\omega) + G_{rep}(\omega)$ with $G_e = (5/4)G_N$.

$$G(\omega) = G_e\phi_a\left(\frac{1}{5Z_a}\sum_{k=1}^{Z_a-1}\frac{i\omega\tau_e Z_a^2}{k^2 + i\omega\tau_e Z_a^2} + \frac{1}{Z_a}\sum_{k=Z_a}^{N_a}\frac{i\omega\tau_e Z_a^2}{2k^2 + i\omega\tau_e Z_a^2}\right) +$$

$$G_e\phi_{bb}\left(\frac{1}{5Z_{bb}}\sum_{k=1}^{Z_{bb}-1}\frac{i\omega\tau_e Z_{bb}^2}{k^2 + i\omega\tau_e Z_{bb}^2} + \frac{1}{Z_a}\sum_{k=Z_{bb}}^{N_{bb}}\frac{i\omega\tau_e Z_{bb}^2}{2k^2 + i\omega\tau_e Z_{bb}^2}\right) +$$

$$G_N(1+\alpha)\phi_a\int_0^1(1-\phi_a s_a)^\alpha\frac{i\omega\tau_a(s_a)}{1+i\omega\tau_a(s_a)}\,ds_a +$$

$$G_N(1+\alpha)\phi_{bb}^{\alpha+1}\int_0^{s_d}(1-s_{bb})^\alpha\frac{i\omega\tau_{bb}(s_{bb})}{1+i\omega\tau_{bb}(s_{bb})}\,ds_{bb} +$$

$$G_N(\phi_{bb}(1-s_d))^{\alpha+1}\sum_{q=odd}\frac{8}{\pi^2 q^2}\frac{i\omega\tau_d(s_d)}{q^2 + i\omega\tau_d(s_d)} \quad (10)$$

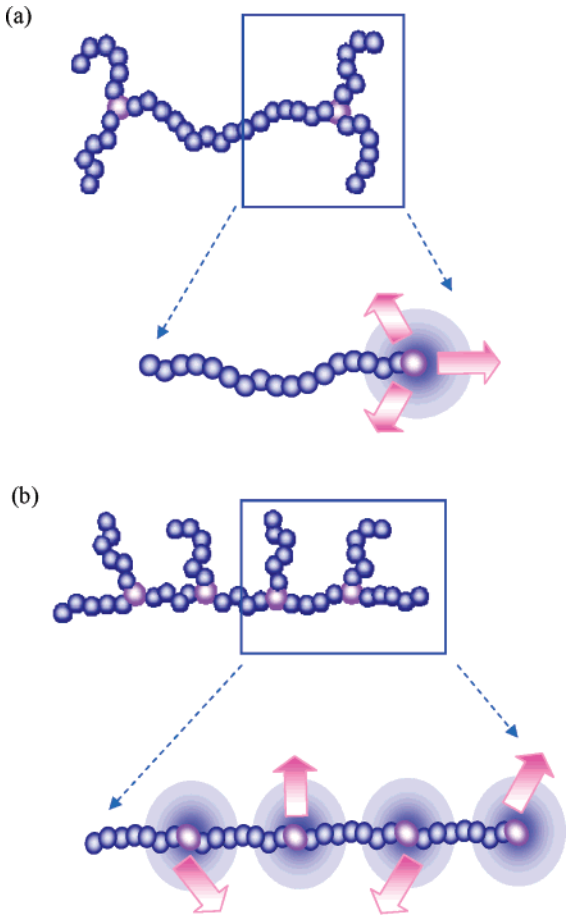

Figure 5. Illustration of the half-arm fluctuating motion executed (a) by a H-shaped and (b) by a comb polymer.

Comparisons between Experiment and Theory. The storage and loss moduli of two 1,4-polyisoprene H-shaped polymers from McLeish et al.[12] are compared with predictions from the current model in Figure 6. The structural characteristics of the H-shaped polymers are provided in Table 2. In their earlier analysis McLeish et al. reported best fit G_N, M_e, and τ_e values of 0.52 [MPa], 4000−5000 [g/mol], and 7 $\times 10^{-6}$ [s], respectively. The model parameters used in the current analysis are $M_{ef} = 4200$ [g/mol], $\tau_{ef} = 7.4 \times 10^{-6}$ [s], the same as for the earlier asymmetric star PI, and $G_{Nf} = 0.5$ [MPa], which is similar to the plateau modulus reported by McLeish et al., but about 20% lower than the value deduced earlier for symmetric and asymmetric star PI.[15,28] The value of G_N determined from the relation, $G_N = \rho RT/(5/4)M_e = 0.42$ [MPa] for $M_{ef} = 4200$ [g/mol], which is in better accord with the best-fit plateau modulus value, G_{Nf}, used here. Agreement between theory and experiment is comparable to that achieved without polydispersity corrections in earlier works by McLeish et al.[12] and by Frischknecht et al.[14] Significantly, in the current case the branch point diffusivity is obtained self-consistently from the theory. The value of the branch point hopping parameter, $p^2 = 1/Z_{bb} = 0.038$, deduced from our analysis is also close to the best fit value $p^2/q = 1/24$ obtained in the earlier work,[12−14] explaining the authors conclusion that $p^2 = 1/12$ for these polymers. As in the previous work, we anticipate that inclusion of a correction for polydispersity will improve agreement between model predictions and experiment; however for reasons outlined earlier, we do not pursue these effects here. Thus, the proposed model shows a capability to reflect the effect of different arms on the relaxation dynamics.

Comparisons between theory and LVE data for combs provide an even more challenging test for the proposed relationship between p^2 and backbone entanglement density. Storage and loss moduli of three different polybutadiene comb polymers from Daniels et al.[13] are compared with model predictions in Figure 7a−d. While the arm molecular weights of the combs are similar, the backbone molecular weight increases down the sequence (see Table 2). Also, while PBC8 has relatively small number of branch points along its long backbone, the other two combs have a significantly larger number of branches. These polymers therefore allow both the effect of backbone molecular weight and number of branch points to be examined. The same model parameters, $M_{ef} = 1850$ [g/mol], $\tau_{ef} = 1.1 \times 10^{-7}$ [s], and $G_{Nf} = 1.6$ [MPa], are used for each of the three combs. These values are comparable to those found in earlier studies of entangled 1,4-polybutadiene linear and symmetric star polymers.[28,29] The value of G_N determined from the relation $G_N = \rho RT/(5/4)M_e = 0.96$ [MPa], for $M_{ef} = 1850$ [g/mol], is nonetheless substantially lower than that deduced from the model fits, again consistent with our earlier observations for linear and symmetric star 1,4-polybutadiene.[28,29]

It is apparent from Figure 7a,b that model predictions are in reasonably good agreement with experimental data for PBC5 and PBC9. Correct predictions for the shape of $G'(\omega)$ and depth of the $G''(\omega)$ minimum in the

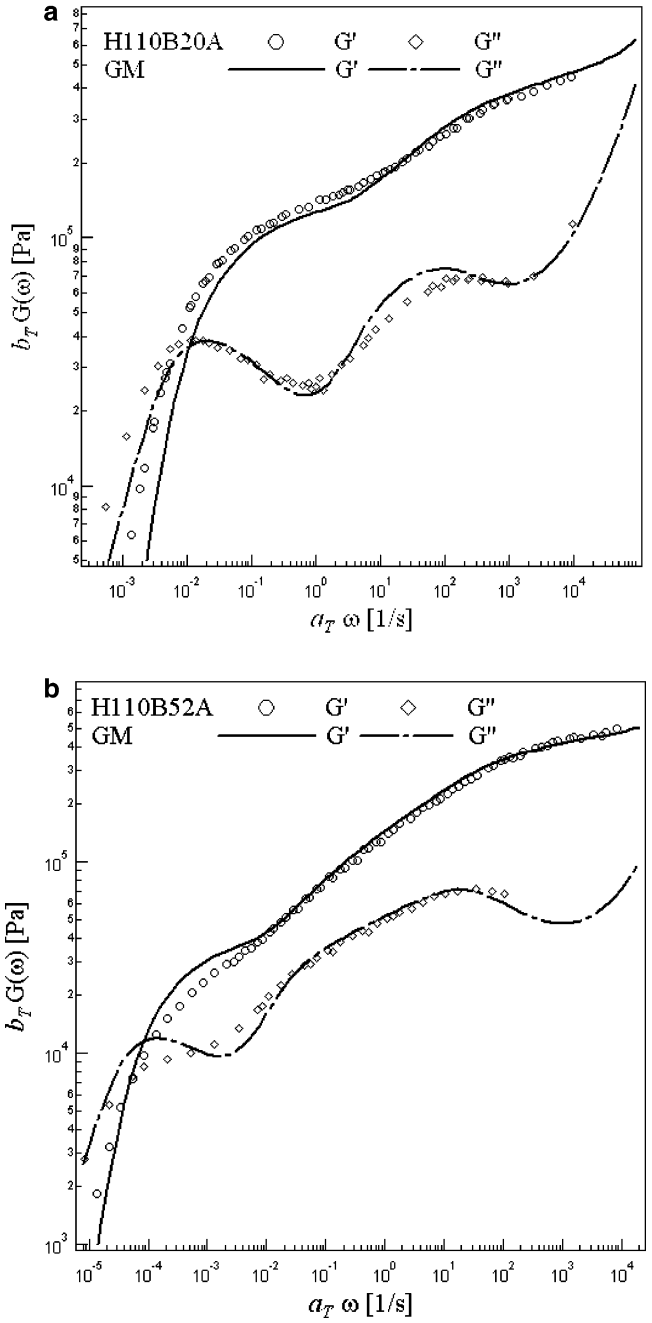

Figure 6. (a) Experimental and theoretical dynamic moduli, $G'(\omega)$ and $G''(\omega)$, for a polyisoprene H-shaped polymer (H110B20A). Symbols are the measured data,[12] and lines are theoretical predictions based on the molecular weight and architecture reported by the authors in ref 12. (b) $G'(\omega)$ and $G''(\omega)$, for a polyisoprene H-shaped polymer (H110B52A). Symbols are the measured data,[12] and lines are theoretical predictions based on the molecular weight and architecture reported by the authors in ref 12.

rubbery plateau region as well as the $G'(\omega) - G''(\omega)$ crossover point in the high-frequency Rouse regime simultaneously attest to the accuracy of the model parameters and imply that the suggested fluctuation mode (Lq mode) correctly captures the physics of branch point motion in comb polymers.

Figure 7c summarizes model predictions and experimental data for PBC8. It is immediately apparent that the model predictions deviate substantially from the measured moduli over the entire frequency range. The predicted depth of the $G''(\omega)$ minimum at high frequency is in particular much larger than what is observed experimentally. One explanation of these observations is that the architecture of PBC8 anticipated from synthesis is different from that of the actual polymer. Specifically, for comb polymers with long backbone lengths and relatively small number of branch points, the placement of branch points relative to the end can significantly alter the effective backbone length.[13,30] If the first branch is placed at a distance from the ends comparable to the branch length, a significant portion of the backbone will relax by arm retraction on a time scale of order $\tau_{a,B}$ by a mechanism analogous to the Y-shaped asymmetric stars considered earlier. This means that the comb may be properly visualized as an H-shaped polymer with an extra branch near the midpoint of the backbone. If the spacing between adjacent branch points is assumed to be equal, the average spacing between branch points is $M_{bb}/(q + 1) = 29.6$ [g/mol], which is evidently close to the arm molecular weight M_a, confirming the H-shaped structure. The effective backbone molecular weight and the effective volume fraction of arms can then be computed as $M_{bb,eff} = M_{bb} - 2M_a$ and $\phi_{bb,eff} = M_{bb,eff}/(M_{bb} + qM_a) = 1 - \phi_{a,eff}$, respectively.

Table 2. Characterization Information for All Branched Polymers Used in This Study

branched polymers	M_a [g/mol]	M_{bb} [g/mol]	q	q_{model}
polyisoprene[12]				
H110B20A	20.0×10^3	111×10^3	2	2
H110B52A	52.5×10^3	111×10^3	2	2
polybutadiene[13]				
PBC5	11.9×10^3	63.9×10^3	8.6	8
PBC9	20.1×10^3	81.8×10^3	7.7	8
PBC8	22.7×10^3	118.5×10^3	3.4	3
polystyrene[31]				
C732	25.7×10^3	860×10^3	26	26
C742	47.0×10^3	860×10^3	29	29
polybutadiene[32]				
P1589	20.0×10^3	83×10^3	2	2
P1508	20.2×10^3	42×10^3	2	2

Figure 7d compares predictions of the generalized model with the experimental data. Model parameters are the same for all other combs, but the analysis is based on the assumption that PBC8 is in reality H-shaped with an extra arm near the center. The much better agreement evident from the figure, particularly the depth of the $G''(\omega)$ minimum at high frequency, appears to confirm our diagnosis of PBC8. The quality of predictions in the lower frequency region is still not quantitative, however. Again, we believe these details are best left to future work that address the role of polydispersity in both the length of the branches and backbone chains and takes into account the near certain distributions in placement of the first branch relative to the chain ends and branch spacing along the comb backbone.

Next we compare dynamic moduli of two different polystyrene comb polymers reported by Roovers and Graesesely[31] with the generalized model predictions in order to examine the effect of arm molecular weight and number of branch points on relaxation dynamics. The number of branch points for both polymers is much larger than for the PBC materials, so uncertainties about the placement of the first branches relative to the

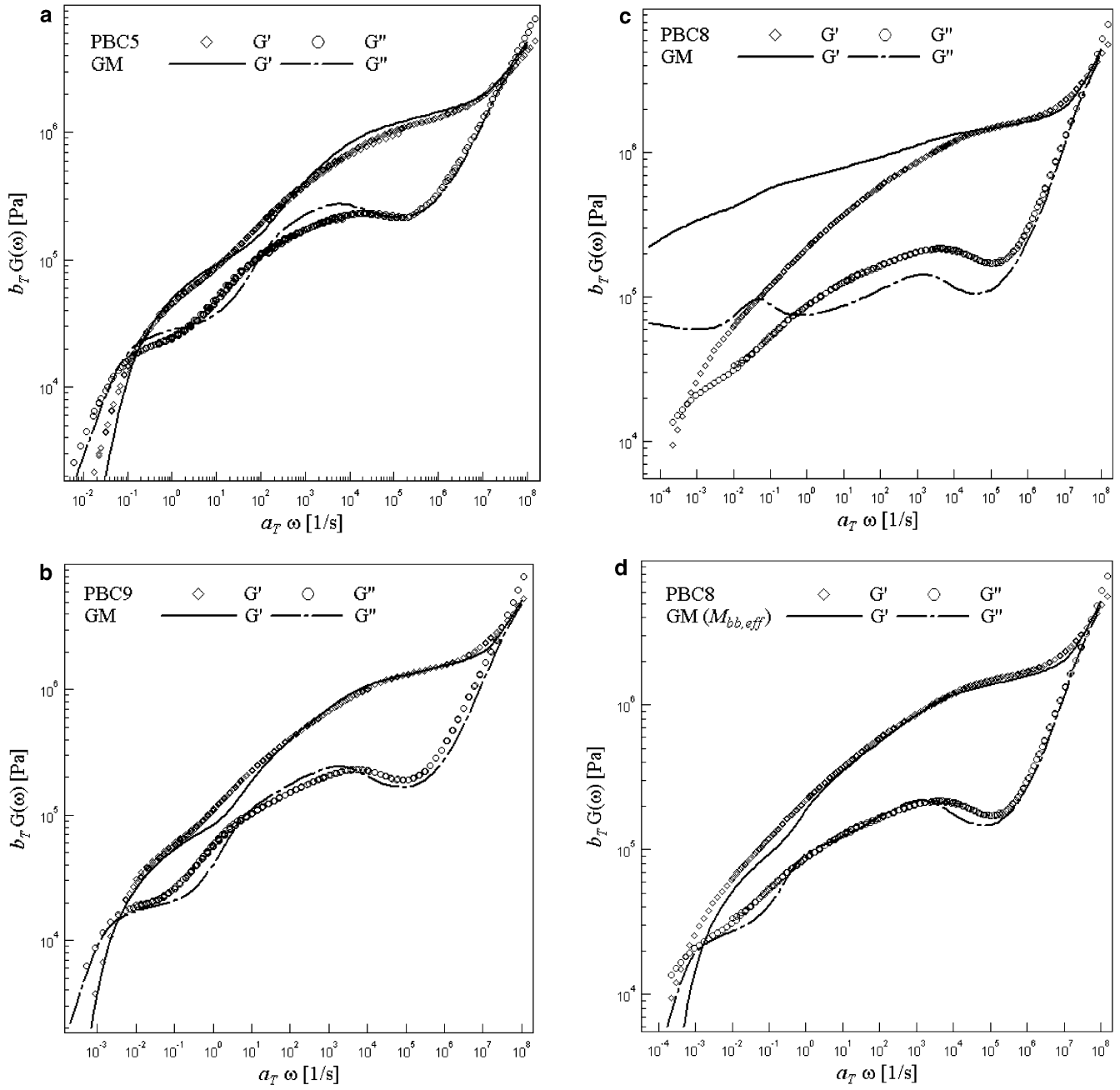

Figure 7. (a) $G'(\omega)$ and $G''(\omega)$, for a polybutadiene comb polymer (PBC5). Symbols are the measured data,[13] and lines are model predictions based on the molecular weight and architecture reported by the authors in ref 13. (b) Dynamic moduli, $G'(\omega)$ and $G''(\omega)$, for a polybutadiene comb polymer (PBC9). Symbols are the measured data,[13] and lines are model predictions based on the molecular weight and architecture reported by the authors in ref 13. (c) Dynamic moduli, $G'(\omega)$ and $G''(\omega)$, for a polybutadiene comb polymer (PBC8). Symbols are the measured data,[13] and lines are model predictions based on the molecular weight and architecture reported by the authors in ref 13. (d) Dynamic moduli, $G'(\omega)$ and $G''(\omega)$, for a polybutadiene comb polymer (PBC8) are compared. Symbols are the measured data,[13] and lines are predictions based on the effective backbone molecular weight ($M_{bb,eff}$) discussed in the text.

ends of the backbone are likely unimportant. Also, the effective volume fraction of backbone in these polymers can be independently estimated from the ratio of the secondary plateau modulus G_{II} and the rubbery plateau modulus G_N at the $G''(\omega)$ local minimum as $(G_{II}/G_N)^{1/\alpha} = \phi_{bb,est}$.[16,28] The estimated backbone volume fractions for C732 and C742 with $\alpha = 4/3$ are $\phi_{bb,est} = 0.57$ and $\phi_{bb,est} = 0.39$, respectively. These values are identical to those determined from the molecular weights and architecture characterization information provided by Roovers and Graesesely.[31]

Model predictions are compared with experimental data in Figure 8a,b. The best-fit model parameters for both polymers are $M_{ef} = 15\,000$ [g/mol], $\tau_{ef} = 4.0 \times 10^{-4}$ [s], and $G_{Nf} = 0.3$ [MPa]. These values should be compared with the measured values of G_N and M_e, $G_N = 0.2$ [MPa] and $M_e = 18\,000$ [g/mol], reported by Roovers and Graessley,[31] and with the best-fit model parameters, $M_{ef} = 14\,470$ [g/mol], $\tau_{ef} = 9.22 \times 10^{-4}$ [s], and $G_{Nf} = 0.22$ [MPa], for polystyrene linear polymers at the same reference temperature reported by Likhtman and McLeish.[27] Again, if we take $M_{ef} = 15\,000$ [g/mol], the plateau modulus deduced from $G_N = \rho RT/(5/4)M_e = 0.19$ [MPa] is moderately lower than the fitted value obtained under the assumption that M_{ef} and G_{Nf} are independent model parameters. It is apparent from

the figures that the storage and loss moduli of both comb polymers are in good to excellent agreement with our model predictions over the entire frequency range. It is again important to point out that no adjustments of the molecular weights reported by the authors is needed, and polydispersity effects have not been taken into account in this analysis.

Two polybutadiene multiarm polymers studied by Islam et al.[32] have three equal-length arms at each branch point. Dynamics of these polymers are expected to be similar to those of H-shaped polymers, but the larger number of arms per branch point could lead to additional complexities. In addition, both backbones contain more 1,2-polybutadiene isomer content than the arms, so two values of M_e could in principle be needed. Figure 9a,b compares the model predictions with experimental data. The best-fit model parameters, $M_{ef} = 2100$ [g/mol], $\tau_{ef} = 3.0 \times 10^{-7}$ [s], and $G_{Nf} = 1.5$ [MPa], are fixed for all comparisons. Because of the larger number of arms per branch point, Figure 9a compares the theoretical predictions both with the *Lq* and *Sq* early fluctuation modes. It is apparent from the figure that the model predictions based on the *Sq* mode are in better agreement with the experimental data, but the agreement is still best described as qualitative. On the other hand, Figure 9b shows that the generalized model with *Lq* mode early fluctuations quantitatively reproduces the experimental results for P1508 over the entire range of frequency studied. That no consideration of polydispersity in arm or cross-bar molecular weights and no explicit accounting for the heterogeneity of the 1,2-/1,4-isomer content of the arms and cross-bars are required indicates that these effects are likely unimportant for this polymer. Their role in the P1589 predictions is clearly an issue for further research. The observed dominance of the *Lq* mode for P1508 is also surprising at first glance, given the qualitative similarity to the H-polymer architecture. This finding can be rationalized, however, by considering the relative short size of the cross-bar relative to the arms. This means that motional constraints produced by the two large friction blobs at the chain ends will be more highly correlated than in the case of a pom-pom or H-shaped polymer with longer backbone. Thus, the fluctuating motion of the two friction blobs will more closely resemble motion of a branch point in comb polymers, reiterating our earlier point that several structural factors such as the number of branch point, the placement of branch points relative to the backbone ends, and the entanglement density of the unrelaxed section of the backbone can all combine to complicate fluctuation and terminal relaxation dynamics of architecturally complex molecules.

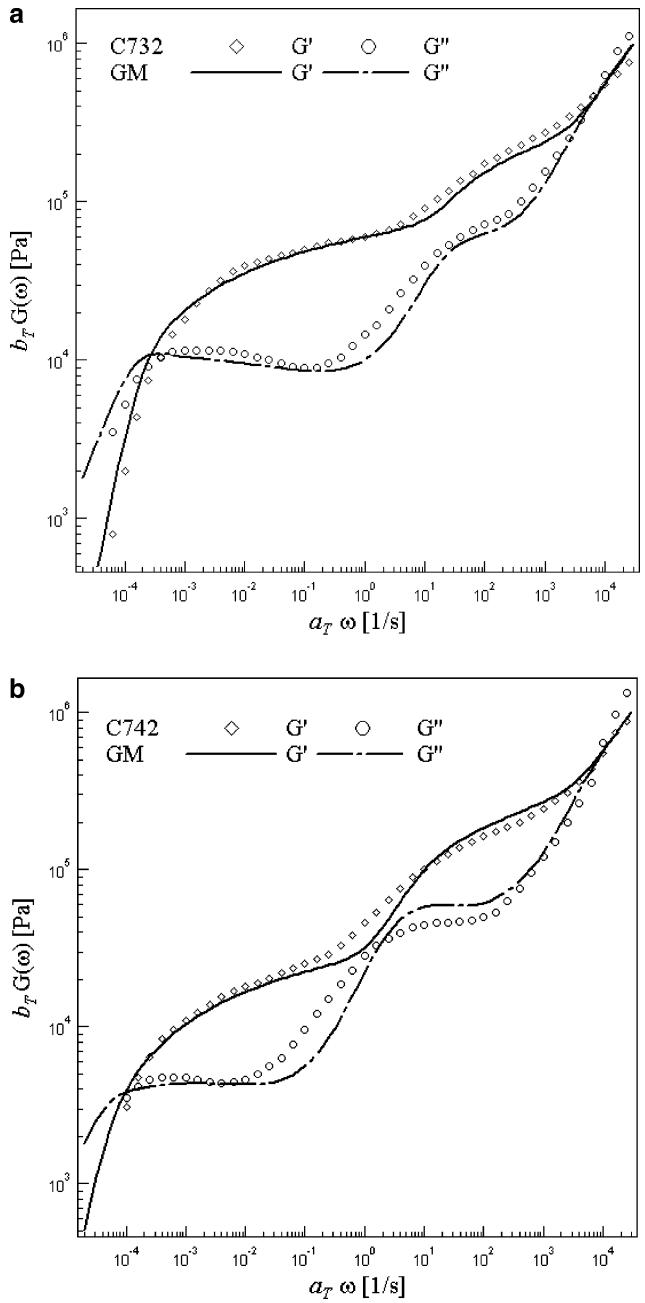

Figure 8. (a) Comparison of experimental and theoretical $G'(\omega)$ and $G''(\omega)$ for a polystyrene comb polymer (C732). Symbols are the measured data,[31] and lines are predictions based on the molecular weight and architecture reported by the authors in ref 31. (b) Comparison of experimental and theoretical $G'(\omega)$ and $G''(\omega)$ for a polystyrene comb polymer (C742). Symbols are the measured data,[31] and lines are predictions based on the molecular weight and architecture reported by the authors in ref 31.

Conclusions

Stress relaxation dynamics of several branched polymers were compared with the predictions of a tube-based theory to evaluate a recent proposal for branch point motion in architecturally complex polymers. The proposed model takes into account both the localized drag force exerted on the branch point of a hierarchically branched molecule by arms attached directly to it and the distributed drag of chains coupled with the molecule by entanglements. An important prediction is that if the random coil size of relaxed molecular segments connected to a polymer branched junction (e.g., $R_{g,\mathbf{B}}$ in an $A_2\mathbf{B}$ asymmetric three-arm star polymer with $M_{w,A} \gg M_{w,\mathbf{B}}$) is larger than the undilated tube diameter a_0, the branch point can only move a small distance $\delta = (ap)$ of order $a_0/\sqrt{Z_{A,R}}$ during each relaxation cycle of the **B** arms, i.e. $D_{bp} = \delta^2/2\tau_{a,\mathbf{B}} = a_0^2/(2Z_{A,R}\tau_{a,\mathbf{B}})$. When this formula is integrated into tube models for branched molecules, it yields a self-consistent theory for describing linear viscoelasticity (LVE) of any branched molecules. Without any artifices, such as adhoc adjustments of the measured molecular weights, arm functionality, or Colby−Rubinstein dilution exponent,[26] we find that this theory yields LVE predictions that are in good agreement with published data from many groups. The

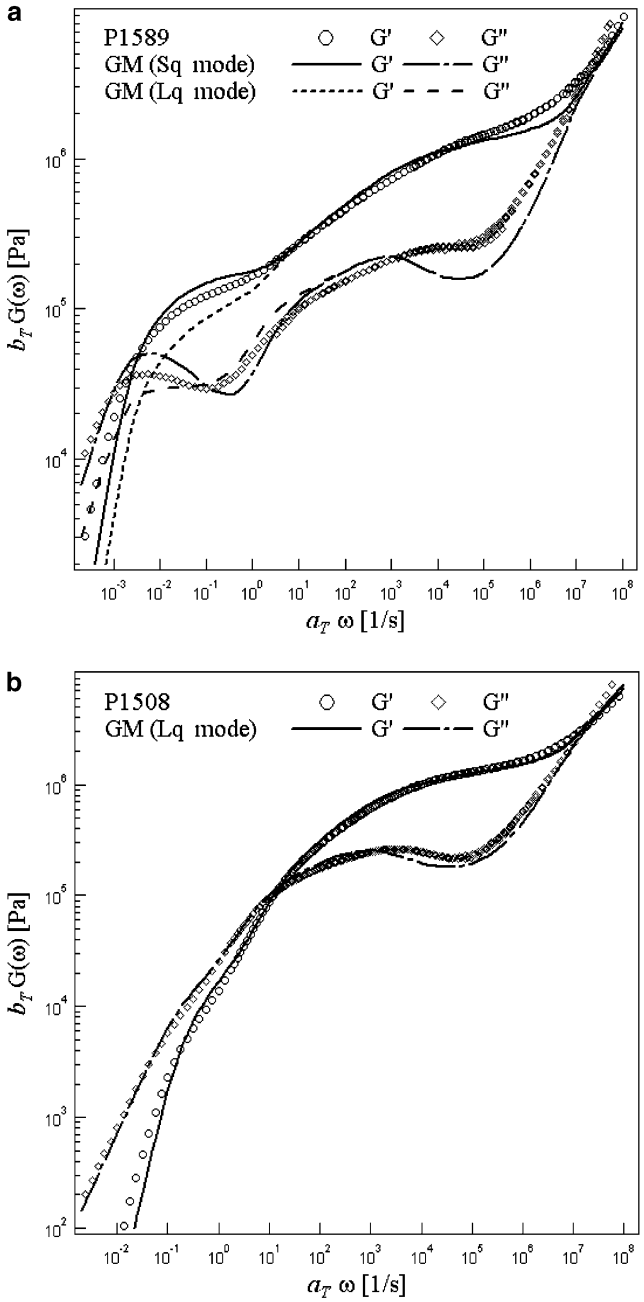

Figure 9. (a) $G'(\omega)$ and $G''(\omega)$ for a 1,4-polybutadiene multiarm polymer (P1589). Symbols are the measured data,[32] and lines are theoretical predictions based on the molecular weight and architecture reported by the authors in ref 32. (b) $G'(\omega)$ and $G''(\omega)$ for a 1,4-polybutadiene multiarm polymer (P1508). Symbols are the measured data,[32] and lines are theoretical predictions based on the molecular weight and architecture reported by the authors in ref 32.

theory can be improved by taking into account several additional details, e.g., the finite polydispersity of the arms and backbone length and distribution of branch spacing and branch placement relative to the chain ends; we do not pursue these effects here. An area of continuing concern with all mathematical models, including the current one, based on the dynamic dilution *ansatz*, is the small, but consistent, difference between values of the entanglement molecular weight deduced from the formula $M_e = \rho RT/(5/4)G_N$ and that determined by considering M_e and G_N as independent model parameters. It is possible that this discrepancy stems from the still uncertain value of the prefactor in the retraction potential,[8,17,20,33] but more work is clearly needed to determine this.

Acknowledgment. Financial support from the National Science Foundation (Grant DMR0237052) and the Department of Energy Basic Science Program (Grant DE-FG02-02ER4600) is gratefully acknowledged.

Note Added after ASAP Publication. This article was published ASAP on November 10, 2005. Changes have been made in equations 4 and 8. The correct version was posted on November 17, 2005.

References and Notes

(1) de Gennes, P. G. *J. Chem. Phys.* **1971**, *55*, 572.
(2) Doi, M.; Edwards, S. F. *The Theory of Polymer Dynamics*; Oxford University Press: Oxford, 1986.
(3) Meissner, J. *J. Appl. Polym. Sci.* **1972**, *16*, 2877.
(4) Laun, H. M. *J. Rheol.* **1986**, *30*, 459.
(5) Minoshima, W.; White, J. *J. Non-Newt. Fluid Mech.* **1986**, *19*, 275.
(6) Scheve, B. J.; Mayfeild, J. W.; DeNicola, A. J. U.S. Patent 4916198, Himont Inc., 1990.
(7) Doi, M.; Kuzuu, N. Y. *J. Polym. Sci., Lett.* **1980**, *18*, 775.
(8) Pearson, D. S.; Helfand, E. *Macromolecules* **1984**, *17*, 888.
(9) Ball, R. C.; McLeish, T. C. B. *Macromolecules* **1989**, *22*, 1911.
(10) Marrucci, G. *J. Polym. Sci., Polym. Phys. Ed.* **1985**, *23*, 159.
(11) Milner, S. T.; McLeish, T. C. B. *Macromolecules* **1997**, *30*, 2159.
(12) McLeish, T. C. B.; et al. *Macromolecules* **1999**, *32*, 6738.
(13) Daniels, D. R.; McLeish, T. C. B.; Crosby, B. J.; Yong, R. N.; Fernyhough, C. M. *Macromolecules* **2001**, *34*, 7025.
(14) Frischknecht, A. L.; Milner, S. T.; Pryke, A.; Young, R. N.; Hawkins, R.; McLeish, T. C. B. *Macromolecules* **2002**, *35*, 4801.
(15) Lee, J. H.; Fetters, L. J.; Archer, L. A. *Macromolecules* **2005**, *38*, 4484.
(16) Archer, L. A.; Juliani *Macromolecules* **2004**, *37*, 1076.
(17) Helfand, E.; Pearson, D. *J. Chem. Phys.* **1983**, *79*, 2054.
(18) Rubinstein, M.; Colby, R. H. *J. Chem. Phys.* **1988**, *89*, 5291.
(19) McLeish, T. C. B. *J. Rheol.* ***2003***, *47*, 177.
(20) Batra, A.; Cohen, C.; Archer, L. A. *Macromolecules*, **2005**, *38*, 7174.
(21) Gell, C. B.; Graessley, W. W.; Efstratiadis, V.; Pitsikalis, M.; Hadjichrstidis, N. *J. Polym. Sci., Part B: Polym. Phys.* **1997**, *35*, 1943.
(22) Juliani; Archer, L. A. *Macromolecules* **2002**, *35*, 6953.
(23) Juliani; Archer, L. A. *Macromolecules* **2002**, *35*, 10048.
(24) Watanabe, H.; Ishida, S.; Matsumiya, Y.; Inoue, T. *Macromolecules* **2004**, *37*, 1937. Watanabe, H.; Ishida, S.; Matsumiya, Y.; Inoue, T. *Macromolecules* **2004**, *37*, 6619.
(25) Frischknecht, A. L.; Milner, S. T. *Macromolecules* **2000**, *33*, 9764.
(26) Colby, R. H.; Rubinstein, M. *Macromolecules* **1990**, *23*, 2753.
(27) Likhtman, A. E.; McLeish, T. C. B. *Macromolecules* **2002**, *35*, 6332.
(28) Lee, J. H.; Fetters, L. J.; Archer, L. A.; Halasa, A. F. *Macromolecules* **2005**, *38*, 3917.
(29) Lee, J. H.; Archer, L. A. *Macromolecules* **2002**, *35*, 6687.
(30) Kapnistos, M.; Vlassopoulus, D.; Roovers, J.; Leal, L. G. *Macromolecules* **2005**, *38*, 7852.
(31) Roovers, J.; Graessely, W. W. *Macromolecules* **1981**, *14*, 766.
(32) Islam, M. T.; Juliani; Archer, L. A.; Varshney, S. K. *Macromolecules* **2001**, *34*, 6438.
(33) Shanbhag, S.; Larson, R. G. *Phys. Rev. Lett.* **2005**, *94*, 076001.

MA051856X